

Determination of electromagnetic properties of steel for prediction of stray losses in power transformers

Leonardo ŠTRAC^{1,*}, Damir ŽARKO²

¹Končar Power Transformers Ltd., Research and Development Department, Zagreb, Croatia

²Department of Electrical Machines, Drives, and Automation, Faculty of Electrical Engineering and Computing, University of Zagreb, Zagreb, Croatia

Received: 06.01.2013

Accepted/Published Online: 25.08.2013

Printed: 28.08.2015

Abstract: This paper introduces a method for determination of equivalent linear electromagnetic parameters (constant complex permeability and electrical conductivity) of nonlinear magnetic steel, which can be used in a time-harmonic finite-element simulation to yield the same losses in the volume of that material as the measured ones. The conductivity and the static hysteresis loop of the steel have been measured, from which complex permeability as a function of flux density has been extracted. The indirect measurement of losses in various samples of nonmagnetic and magnetic steel has been carried out using a physical model of a transformer core with a coil. The 3D model of the core has been made with finite-element software and combining it with evolutionary optimization the equivalent constant complex permeability and conductivity of each sample have been found, which yield the equality of measured and calculated losses in the sample. Thus, calculated equivalent material parameters have been implemented in 3 finite-element models of transformers of various power ratings in order to determine the share of hysteresis losses in the total amount of losses in structural parts of transformers. The results have been compared with the measurement and the reasons for discrepancies have been explained.

Key words: Transformers, steel, magnetic losses, eddy currents, hysteresis, permeability, finite element methods, optimization

1. Introduction

One of the materials commonly used in power transformers in electric power transmission is plain magnetic steel. The steel is used for clamping systems, tanks, and other construction parts of the transformer [1]. Since construction parts do not participate in the energy conversion, the electromagnetic properties of plain steel are rarely considered. Nevertheless, the transformer components made of solid steel are not absolutely passive because of the transformer's stray field, which induces eddy currents in construction parts and causes so-called additional losses [1]. The additional losses are typically a small part of the total losses in a transformer, but they should not be ignored because if the local additional losses are too high, it can lead to local overheating, damaging of cellulose electric insulation, and degradation of mineral oil [2].

Plain magnetic steel is used in power transformers for its low price and excellent mechanical properties. However, it is a very complex material from the electromagnetic point of view with nonlinear magnetization characteristic, hysteresis, variation of electromagnetic properties due to mechanical processing, and often

*Correspondence: leonardo.strac@siemens.com

anisotropy. Moreover, the chemical composition of plain steel is not guaranteed by the manufacturer and it can vary from shipment to shipment. For those reasons the eddy current and hysteresis losses in the plain steel are very unpredictable. Besides plain magnetic steel, nonmagnetic steel is commonly used in critical places in the transformer like clamping systems, parts of the tank, tank covers, lead turrets, etc. [1]. While relative permeability of nonmagnetic steel is very close to the relative permeability of air, its exact value is still unknown as well as its specific electrical conductivity. The reason for that is the variation of its magnetic properties due to mechanical processing like welding or machining, in which case its permeability can rise significantly [3].

The exact values of additional losses in the specific parts of the transformer are very difficult to measure, so they are usually estimated from the total measured losses during the short-circuit test of the transformer. The losses depend on the flux density on the surfaces of the construction parts.

One method that can be used for measuring magnetic flux density is the thin film sensor method [4,5]. By using thin film sensors it is possible to measure flux density in the core, tank shields, surface of the clamping system parts, and surface of the tank. However, for calculation of eddy current losses using the measured values of flux density, one still needs to know the electromagnetic parameters of the tank and clamping system materials. Besides that, for measurement of flux density in a typical large power transformer, a very high number of sensors are needed to cover all construction parts of the transformer. Such measurements would be very long and expensive with a high danger of electrical breakdown because of the presence of the sensor wires.

There is also a possibility for measuring the losses in various parts of a transformer by using the Poynting vector directly [6]. The advantage of this method is the usage of sensors built from small cube-shaped samples of the same material as the material of the object inside the transformer where the losses should be determined. Because of that, it is not necessary to know the electromagnetic parameters of material where the losses are measured. However, the magnetic field at the location of such sensors in the vicinity of the steel surface of the tank or the core clamp where losses are induced is not exactly the same as the field on the steel surface itself. In addition, a small sample of material cannot give the correct distribution of losses in the large steel surfaces that are common in power transformers. The mechanical processing of the material required for construction of the sensor may also alter its magnetic properties. This sensor is rather complicated and the danger of electrical breakdown is present again.

The additional losses in the power transformers are typically calculated using statistical and empirical methods [2]. For a more thorough investigation of additional losses, a 3D finite-element method (FEM) is typically used. When using the FEM calculation the fundamental data required are electrical and magnetic properties of used materials. Besides that, the use of nonlinear materials requires the execution of simulation in the transient mode, which greatly increases the calculation time and computer resources. In addition, due to the small depth of penetration of the field into the volume of the conductive material, a mesh with a huge number of very small elements would be required. An alternative is to utilize time-harmonic simulation and surface impedance for calculation of eddy current losses.

The purpose of this paper is to investigate the possibility of using linear time-harmonic simulation with a surface impedance approach for calculation of stray losses in power transformers where equivalent electromagnetic properties of nonlinear steel (constant relative permeability and conductivity) are determined from measurements of losses performed on samples of various materials.

The method for determination of equivalent linear electromagnetic properties of steel combines the differential evolution optimization algorithm and FEM with the aim to calculate the same value of losses using linear time-harmonic simulation in a limited range of flux density as measured in a nonlinear material.

An additional feature is the inclusion of hysteresis losses by means of complex relative permeability, which is often neglected in the literature.

The FEM software used in this article is standard commercially available software.

2. Experimental determination of electromagnetic properties of steel

2.1. Model of a transformer core with coil for measurement of losses caused by alternating magnetic field

The losses in samples made of conducting material caused by stray magnetic field cannot be measured directly. Because of that, a simple model of a transformer core with a coil was constructed to measure the losses in material samples as directly as possible (Figure 1). The samples are inserted between the fixed and the movable part of the core, thus being exposed to the magnetic field passing through the core, which is produced by the current flowing in the winding. The core is intended for measurements at the frequency of 50 Hz and flux density up to 0.6 T in the core with a sample inserted.

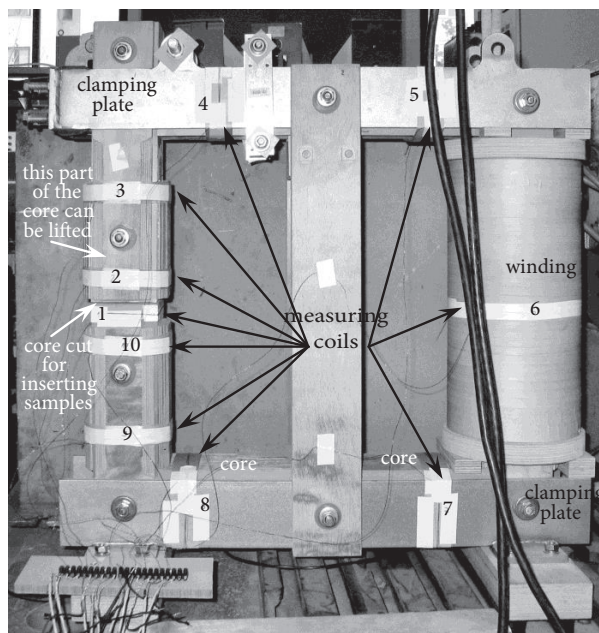


Figure 1. Model of a transformer core with coil for measurement of losses caused by alternating magnetic field.

The core has a square cross-section of 100×100 mm. The size of the core window is 500×500 mm. The core material is cold-rolled silicon steel of 0.3 mm in thickness. On one leg there is a winding with 200 turns and copper conductors with dimensions of 6.2×6.8 mm wound in 4 layers with 3 radial and 1 axial parallel. The other leg is cut and the upper part of the leg is moveable so that various samples can be inserted into the slot. There are 10 measurement coils on the core with 5 turns of $\varnothing 0.30$ mm copper wire for measuring the average flux density in the cross-sections where the coils are located.

Two basic types of measurements have been conducted. The first type is measurements without samples with air gaps of 3, 6, 8, 10, and 15 mm in the core. The purpose of these measurements is to calibrate the calculation of core losses. The second type is measurements with samples; see Table 1.

Table 1. Materials and dimensions of samples.

	Thickness [mm]						
Size [mm]	3	6	8	10	15	20	30
100 × 100							
200 × 200							
400 × 400							
	Copper		Nonmagnetic steel			Magnetic steel	

For accurate determination of losses in the samples it is important to know the exact losses of the core itself. While calculation of the winding losses is trivial, for calculation of the core losses a special method has been developed. Since the core is laminated, nonlinear, anisotropic, and with hysteresis, the method is statistical and takes into account the flux that flows in directions other than the rolling direction of the steel sheets. The flux density component perpendicular to the rolling direction is present due to magnetic field suppression caused by eddy currents induced in the samples inserted between the fixed and movable parts of the core and also due to high magnetic reluctance of the air gap if the movable part of the core is lifted without inserting the sample. In both cases (with samples or with air gap) the flux leakage in the core and the influence of the difference in B-H characteristics of the core silicon steel in the mutually perpendicular axes will be significant.

In order to describe the core losses in a fairly simple manner, a mathematical procedure has been developed that approximates the losses by using the average flux density in the core, which is mainly related to the flux density component oriented in the rolling direction of the sheets, and the factor of flux density dissipation, which is mainly related to the flux density component oriented in the direction perpendicular to the rolling direction. The core loss calculation is derived from measurements conducted with various lengths of the air gap in the core and without any samples inserted. Figure 2 shows the results of six measurements (closed core and air gaps of 3, 6, 8, 10, and 15 mm) as a function of average values of flux densities obtained from all 10 measuring coils (Figure 1). The core losses are obtained by subtracting the winding losses from the total losses measured at the winding terminals. The winding losses are determined using measured current and winding resistance. Each core loss characteristic in Figure 2 is approximated using the polynomial written in the form

$$P_{lossFe} = aB_{mean}^2 + bB_{mean}, \tag{1}$$

where P_{lossFE} are the losses in the core, B_{mean} is the average of flux densities obtained from all 10 measuring coils, and a and b are the coefficients of the polynomial. The coefficients a and b , the accompanying coefficients of determination R^2 , and the factor of flux density dissipation f_{diss} defined as the ratio of maximum B_{core_max} and minimum B_{core_min} flux density obtained from 10 measuring coils are given in Table 2.

The dissipation factor for every size of the air gap is determined as an average value of dissipation factors calculated for each value of the average flux density B_{mean} . Thus, six values of the average dissipation factors are obtained for six sizes of the air gap. The next step is to display coefficients a and b as a function of f_{diss} as shown in Table 2. This table also shows the polynomial fit of a and b calculated as a function of f_{diss} .

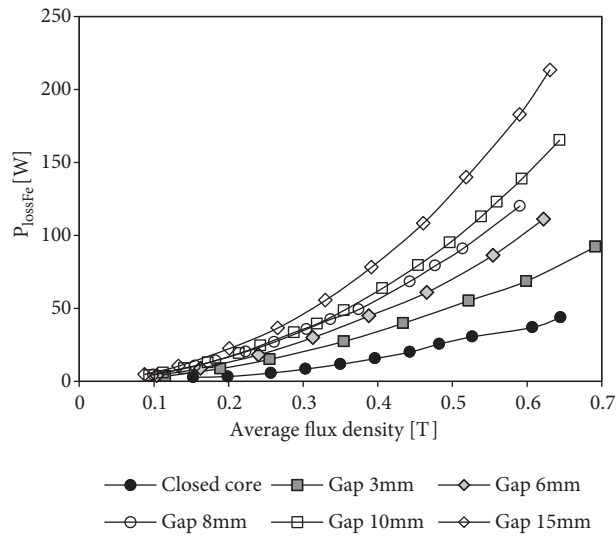


Figure 2. Losses in the model of a transformer core with coil with various air gaps.

Table 2. Coefficients of the polynomial for approximation of the core losses, coefficients of determination, and the factor of flux density dissipation for various sizes of the air gap.

Air gap [mm]	<i>a</i>	<i>b</i>	R ²	<i>f_{diss}</i>
0	103.19	5.87	0.999968	1.10
3	167.71	16.56	0.999279	1.64
6	267.65	9.55	0.999241	2.07
8	332.28	6.86	0.999241	2.32
10	393.45	-0.48	0.999446	2.61
15	544.74	-10.44	0.999277	3.20

The final expressions for the core losses with *a* and *b* replaced by their polynomial fitting functions are given below.

$$\begin{aligned}
 P_{lossFe} &= (117.44f_{diss}^2 - 202.90f_{diss} + 184.52) B_{mean}^2 + \\
 &\quad + (-36.90f_{diss}^2 + 120.57f_{diss} - 81.94) B_{mean}, \text{ for } f_{diss} \leq 1.75 \\
 P_{lossFe} &= (241.85f_{diss} - 231.95) B_{mean}^2 + \\
 &\quad + (-17.50f_{diss} + 45.43) B_{mean}, \text{ for } f_{diss} > 1.75 \\
 f_{diss} &= \frac{B_{core_max}}{B_{core_min}}
 \end{aligned}
 \tag{2}$$

The average deviation between measured and calculated core losses without samples for all six air gap sizes is 0.406 W with the coefficient of determination $R^2 = 0.999506$.

The losses in various samples as a function of the average flux density B_{10} in the core obtained from measuring coil No. 10 (see Figure 1) are shown in Figures 3–6. This measuring coil was chosen as the coil that gives the value of the flux density most relevant to the losses generated in the samples inserted between the fixed and movable sections of the core since its location is very close to the sample, but still far enough to avoid flux density decrease due to flux suppression caused by the sample’s induced eddy currents.

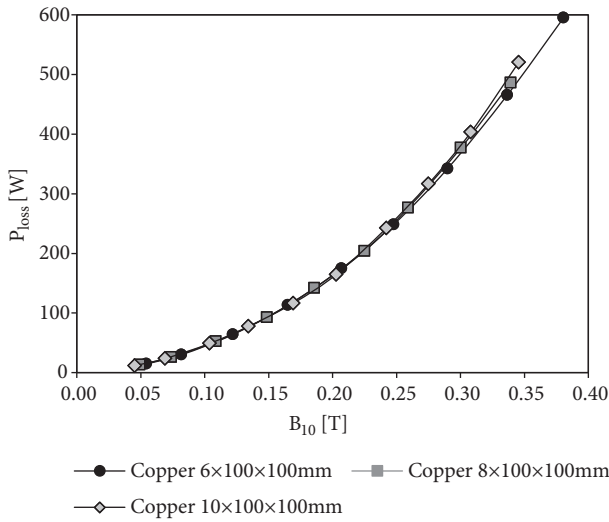


Figure 3. Losses in copper samples with dimensions of 100×100 mm.

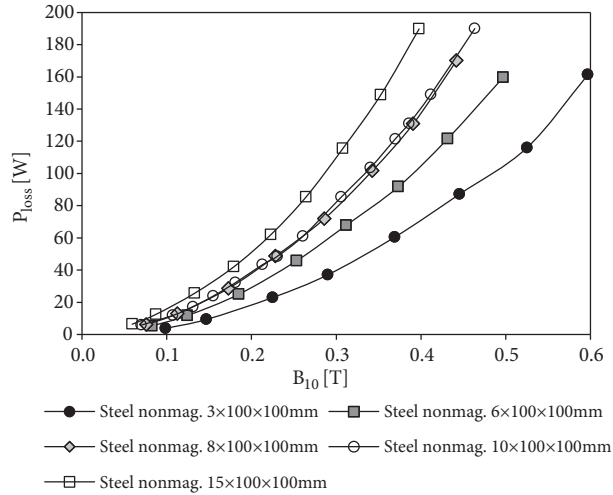


Figure 4. Losses in nonmagnetic steel samples with dimensions of 100×100 mm.

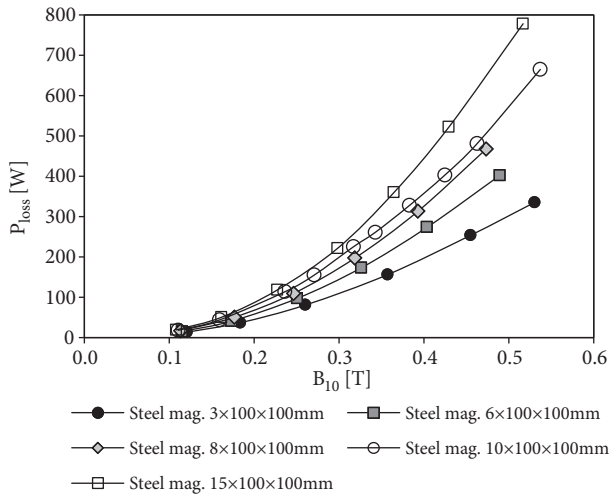


Figure 5. Losses in magnetic steel samples with dimensions of 100×100 mm.

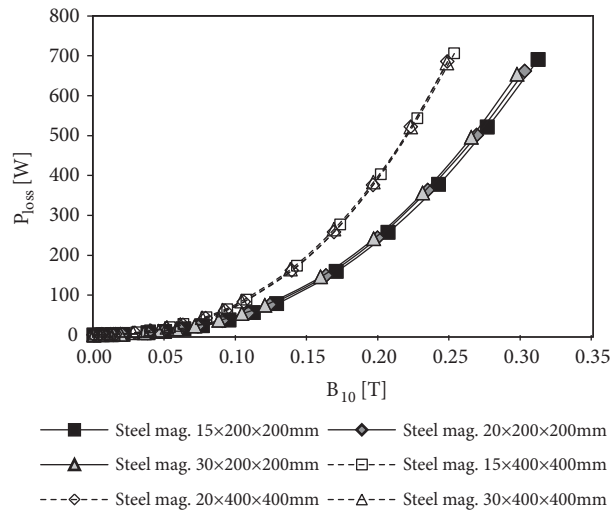


Figure 6. Losses in magnetic steel samples with dimensions larger than 100×100 mm.

The magnetic steel that was used for samples in the experiments is type EN-1.0038, and the nonmagnetic steel is type EN-1.4541. These are the most typical types of steel used for clamping systems and tanks in power transformers.

The losses for copper and nonmagnetic and magnetic steel samples are measured for a flux density range from 0 to 0.6 T. The losses in all cases show quadratic correlation with flux density. For the magnetic steel samples with dimensions of 100×100 mm (Figure 5), the losses increase with sample thickness. This effect is present because magnetic flux penetrates into samples sideways [2]. This occurs because the sample is made of conductive solid material in which the eddy current can flow freely. The eddy currents in the sample are trying to suppress the magnetic flux from the core. Because of that there is hardly any flux in the center of the sample, and all the flux is concentrated on the sample's edges. The final consequence of flux suppression from the sample is the penetration of the magnetic flux into the sample sideways so the relevant direction for the

penetration depth is from the lateral faces of the sample towards the center. For the magnetic steel samples with dimensions larger than 100×100 mm, the magnetic flux penetrates into the 2 largest faces of the samples and in this case the losses increase with the sample width. In the case of samples larger than 100×100 mm, there is similarity in flux suppression to the samples of dimensions 100×100 mm, but with one major difference. Since these samples are larger than the core, the induced eddy current can flow outside the core contours. In this case the relevant direction for the penetration depth is perpendicular to the largest faces.

2.2. Toroidal coils for measurement of hysteresis curves and the curve of the first magnetization

The measurement of hysteresis curves of the magnetic steel is essential for determination of the hysteresis losses, which can be modeled in FEM time-harmonic simulations by means of the complex permeability of the material.

The static and dynamic magnetization and hysteresis curves can differ considerably. However, it is difficult to measure those curves in nonlaminated magnetic material at 50 Hz due to suppression of the magnetic field to the surface. Since lamination of the magnetic steel would change its magnetic properties significantly, the static magnetization and hysteresis curves are obtained to determine the first magnetization curve and the share of the hysteresis losses. For that purpose, 2 toroidal coils with solid cores of nonmagnetic and magnetic steel were built. Both cores have the same dimensions: cross-section of 20×20 mm, and inner and outer diameter of 300 mm and 340 mm, respectively. Every coil has 2 windings. The primary winding has 4000 turns for the nonmagnetic and 1500 turns for the magnetic core, and there are six identical secondary windings, each having 65 turns.

For magnetic steel a family of hysteresis curves has been measured. For every individual curve a set of measurement points that consist of a source current and magnetic flux have been measured for the first and the second quadrant. A referent point for every curve is the point with the maximum current value, so there are curves for 0.05, 0.10, 0.15, 0.2, 0.4, 0.5, 1.0, 1.5, 2.0, 4.0, and 6.5 A respectively. From the measured data it is easy to calculate the magnetic field strength H , flux density B , and real relative permeability μ'_r .

$$H = \frac{N_1 I_1}{l_{mean}}, \quad (3)$$

where N_1 is the primary number of turns, I_1 is the primary current, and l_{mean} is the mean circumference of the core.

$$B = \frac{\Phi}{S} = \frac{\Psi}{N_2 S}, \quad (4)$$

where ψ is the flux linkage, N_2 is the secondary number of turns, and S is the cross-section area of the core.

$$\mu'_r = \left| \frac{B}{\mu_0 H} \right|, \quad (5)$$

where μ_0 is the permeability of vacuum. The end points of every hysteresis curve represent one point of the magnetization curve (Figure 7).

Since the magnetization hysteresis is rather complex to be mathematically defined, there is a common practice of approximation of hysteresis curve by ellipses in FEM software. Considering that the area within the hysteresis curve represents hysteresis energy or work needed to accomplish one full cycle of magnetization, elliptical approximation of hysteresis recreates the hysteresis area. That is accomplished by implementation of imaginary relative permeability μ''_r , which represent the small axis of the ellipse [7], while the big axis of the

ellipse represents real relative permeability μ'_r . Finally, the magnetic loss tangent can be calculated according to

$$\tan \delta_m = \frac{\mu'_r}{\mu''_r} \tag{6}$$

The values of μ'_r , μ''_r , and $\tan \delta_m$ for magnetic steel are shown in Table 3 and Figure 8.

Table 3. Hysteresis energy, real and imaginary relative permeability, and magnetic loss tangent as a function of peak current for magnetic steel.

I_{peak} [A]	B_{sat} [T]	W_{hys} [J]	μ''_r	μ'_r	$\tan \delta_m$
0.05	0.04	0.0015	169.8	450.9	0.37663
0.10	0.12	0.0099	273.1	651.3	0.41931
0.15	0.28	0.0480	595.4	977.8	0.60893
0.20	0.43	0.0857	596.1	1138.5	0.52363
0.40	0.77	0.2307	399.0	1026.9	0.38858
0.50	0.91	0.3342	332.5	916.7	0.36274
1.00	1.20	0.5355	145.4	636.7	0.22836
1.50	1.38	0.7206	85.3	488.9	0.17448
2.00	1.48	0.8419	55.8	392.7	0.14209
4.00	1.65	1.1861	17.9	213.4	0.08381

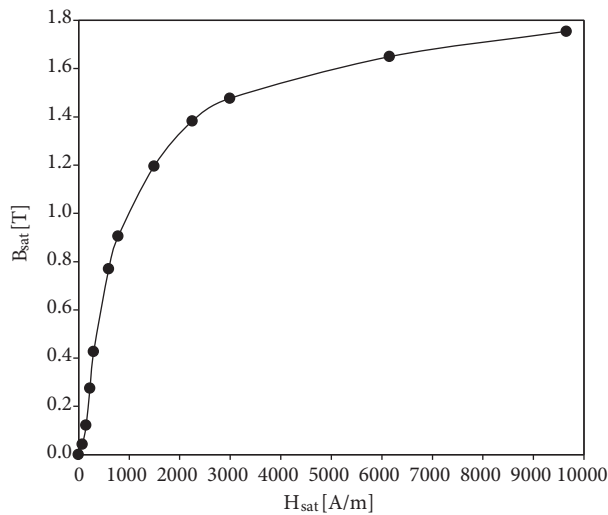


Figure 7. Curve of the first magnetization of solid magnetic steel.

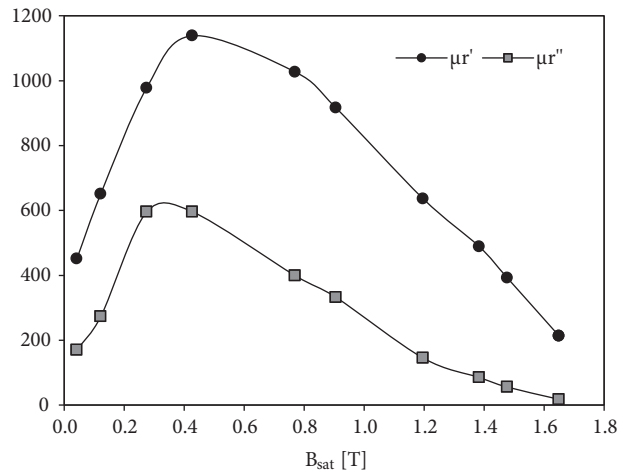


Figure 8. Real and imaginary relative permeability of magnetic steel.

2.3. Rods for measurement of specific conductivity

The manufacturers of plain magnetic and nonmagnetic steel do not provide electric properties of these materials. Moreover, the specific electric conductivity can vary from shipment to shipment. While the measurement of specific electric conductivity of a steel sample does not guarantee that the next shipment is going to have the same value, it gives an insight into the range where the specific electric conductivity can be expected. For that reason, measurements of specific electric conductivity for nonmagnetic and magnetic steel samples of different dimensions have been conducted. The dimensions of various samples and the measurement results are given in Tables 4 and 5, where l is the length, w is the width, and h is the height of the rectangular-shaped rod.

Table 4. Dimensions and resistances of the nonmagnetic steel rods and the specific electric conductivity of nonmagnetic steel at 26.5 °C.

Rod	l [m]	w [m]	h [m]	S[m ²]	R [mΩ]	σ [S/m]
1	0.90	0.01	0.01	1.00E-04	1.78	5.07E+06
2	0.90	0.01	0.01	1.00E-04	1.79	5.03E+06
3	0.91	0.01	0.01	1.00E-04	1.81	5.03E+06
4	0.92	0.01	0.01	1.00E-04	1.82	5.06E+06
5	0.91	0.01	0.01	1.00E-04	1.84	4.94E+06
					Average:	5.02E+06
					St.dev.:	4.77E+04

Table 5. Dimensions and resistances of the magnetic steel rods and the specific electric conductivity of magnetic steel at 26.8 °C.

Rod	l [m]	w [m]	h [m]	S[m ²]	R [mΩ]	σ [S/m]
1	0.91	0.01	0.01	1.00E-04	2.55	3.57E+06
2	0.92	0.01	0.01	1.00E-04	2.79	3.29E+06
3	0.92	0.01	0.01	1.00E-04	2.67	3.44E+06
4	0.92	0.01	0.01	1.00E-04	2.62	3.51E+06
5	0.93	0.01	0.01	1.00E-04	2.58	3.60E+06
6	1.47	0.015	0.005	7.50E-05	3.37	5.81E+06
7	1.46	0.020	0.005	1.00E-04	2.57	5.66E+06
8	1.45	0.030	0.005	1.50E-04	1.97	4.90E+06
					Average:	4.22E+06
					St.dev.:	1.06E+06

3. Determination of equivalent electromagnetic properties of steel

3.1. 3D FEM model of a transformer core with coil for measurement of losses in samples

In the search for the optimal values of equivalent linear electromagnetic parameters of steel samples, it is necessary to have a 3D FEM model for calculation of losses in the samples.

Due to the huge number of calculations that have to be performed during the process of optimization, the model has to be as simple as possible, and yet it has to calculate the losses accurately. For this reason the winding in the model is represented as 4 hollow, conducting, stranded cylinders (for 4 winding layers). The core in the model is made of solid, nonlaminated, isotropic, linear, nonconductive material without hysteresis and with the real relative permeability of 20,000. At the locations of the measurement coils the planes in the cross-section of the core model are defined for monitoring of flux density. Finally, the samples are solid, linear parallelepipeds whose electromagnetic parameters (conductivity and relative complex permeability) can be easily varied by the optimization method. The sample is the only object in the model whose losses are being calculated. The losses calculated from the FEM model are compared with the measured losses with respect to the flux density in the core leg where the sample is located. All calculations are performed in time-harmonic mode. The accuracy of the model is tested on the copper samples of 100 × 100 mm with 6, 8, and 10 mm thickness, because the electromagnetic properties of copper are well known. The average aberration between calculated and measured results for all dimensions and all measurement points is 0.6% with dissipation of 8.0%, which can be considered acceptable. An example of agreement of measured and calculated values is given in Figure 9.

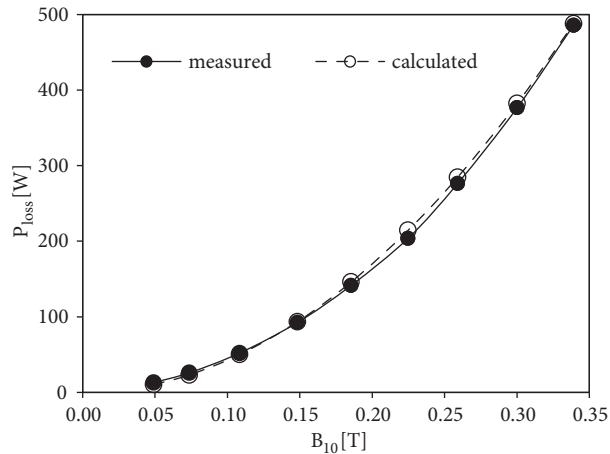


Figure 9. Measured and calculated losses for the copper sample with dimensions of $100 \times 100 \times 8$ mm.

3.2. Determination of equivalent electromagnetic properties of steel using the differential evolution method

Differential evolution (DE) [8] is an optimization algorithm used for determination of equivalent electromagnetic properties of steel. The method is selected because it is fast and robust in finding a global optimum.

For coupling the DE method with FEM calculation, a software interface has been made. The process of optimization works like this: Figures 5 and 6 show how losses in the samples depend on flux density obtained from measurement coil No. 10 placed in the core leg where the sample is located. Every curve is fitted using a second-order polynomial with flux density as a variable given by

$$P_{loss_meas}(B_{meas}) = a_1 B_{meas}^2 + a_2 B_{meas}, \quad (7)$$

where a_1 and a_2 are the polynomial coefficients determined using the least squares fitting method, and B_{meas} is the measured flux density at the location of measuring coil No. 10.

DE creates an initial population of randomly chosen vectors $[\mu'_r, \sigma]$. The imaginary relative permeability μ'_r is not an independent variable in the process because it is linked with μ'_r through the magnetization characteristic of magnetic steel, or it is set as zero in the case of nonmagnetic steel. Each of the vectors $[\mu'_r, \sigma]$ is sent to FEM calculation as the electromagnetic parameters of the sample. The FEM software calculates the value of eddy current and hysteresis losses in sample P_{loss_FEM} and the value of flux density B_{FEM} at the given location in the core (in this case, the location of measuring coil No. 10). Both results are sent back to DE where the flux density from the FEM simulation is used to calculate the measured losses using the polynomial fit function given by Eq. (8). The squared difference between the measured losses calculated using the fit function and the losses calculated using the FEM represents the cost function F_c for that vector of the population.

$$P_{loss_meas}(B_{FEM}) = a_1 \cdot B_{FEM}^2 + a_2 \cdot B_{FEM} \quad (8)$$

$$F_c = [P_{loss_meas}(B_{FEM}) - P_{loss_FEM}]^2 \quad (9)$$

Based on the cost functions for all vectors from that population, DE applies the operators of mutation, crossover, and selection to choose the vectors for the next generation of population. The process is finished when the cost function falls below a given value, for example 10^{-5} .

Using the procedure described above, the determination of equivalent electromagnetic properties has been conducted for every sample, with one exception. Since thickness of the sample does not influence the losses in the case of magnetic steel samples larger than 100×100 mm, for those samples the average values of measured losses for each thickness have been used and 3D models have been made only for $200 \times 200 \times 15$ mm and $400 \times 400 \times 15$ mm.

Table 6 shows the results for the samples of nonmagnetic steel, and Figure 10 shows example of losses calculated with equivalent properties for all measured values of flux density in the core.

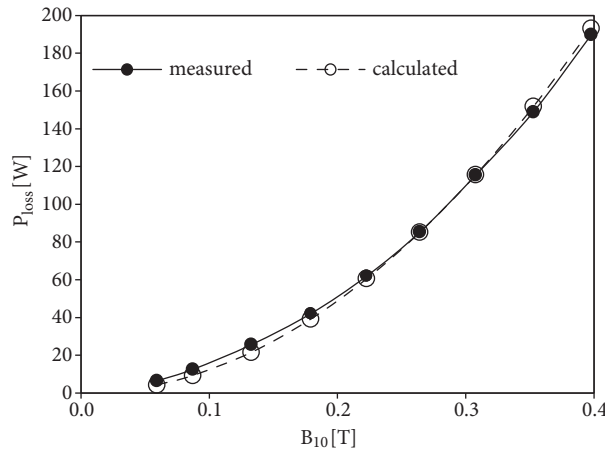


Figure 10. Measured and calculated losses in the nonmagnetic steel sample with dimensions of $100 \times 100 \times 15$ mm.

Table 6. Equivalent electromagnetic properties of nonmagnetic steel samples.

Dim. [mm]	μ'_r	σ [S/m]	F_c
$100 \times 100 \times 3$	4.67	934730	2.79E-05
$100 \times 100 \times 6$	3.53	780121	4.55E-01
$100 \times 100 \times 8$	2.66	852331	1.30E-01
$100 \times 100 \times 10$	2.84	695135	1.27E-01
$100 \times 100 \times 15$	3.78	666551	1.42E-03
Average:	3.50	785774	1.43E-01
St.dev.:	0.80	110769	1.86E-01

Table 7 shows the results for the samples made of magnetic steel, and Figure 11 shows example of losses calculated with equivalent properties for all measured values of flux density in the core for the magnetic steel samples. Finally, Table 8 shows the average aberration and standard deviation between measured values and the values calculated with equivalent linear properties for all measured points per sample.

4. Share of hysteresis losses in the total losses in construction parts of a power transformer

4.1. Transformers for determination of the share of hysteresis losses

For determination of the share of hysteresis losses in the real power transformers, 3 typical transformers from standard factory production have been selected. They are going to be referred to here as transformers A, B, and C. The rated power of the transformers is 40, 150, and 400 MVA, respectively. They are manufactured in series of 20, 1, and 4 units. Table 9 shows the total losses measured during the short-circuit test, and additional losses are calculated by subtracting the ohmic losses and skin-effect losses in the copper from the total losses.

Table 7. Equivalent electromagnetic properties of magnetic steel samples.

Dim. [mm]	μ'_r	μ''_r	$\tan\delta_m$	σ [S/m]	F_c
100 × 100 × 3	5.30	0.32	0.060839	5936147	1.98E-05
100 × 100 × 6	11.28	0.69	0.061426	5789264	9.14E-05
100 × 100 × 8	13.16	0.81	0.061614	6033657	1.67E-04
100 × 100 × 10	14.24	0.88	0.061722	5484592	2.86E-13
100 × 100 × 15	25.56	1.61	0.062901	6044433	6.89E-12
200 × 200 × 15	103.55	7.54	0.072794	5541466	1.45E-13
400 × 400 × 15	267.28	27.71	0.103660	5493468	3.62E-03
			Average:	5760432	5.56E-04
			St.dev.:	252428	1.35E-03

Table 8. Average aberration and standard deviation between measured and calculated point for different samples.

Steel	Dim. [mm]	Avg. aberr.	St. dev.
Nonmag.	100 × 100 × 3	-4.9%	5.1%
Nonmag.	100 × 100 × 6	-7.1%	7.4%
Nonmag.	100 × 100 × 8	-7.5%	8.8%
Nonmag.	100 × 100 × 10	-9.7%	9.9%
Nonmag.	100 × 100 × 15	-12.1%	18.4%
Mag.	100 × 100 × 3	4.2%	9.3%
Mag.	100 × 100 × 6	5.4%	12.8%
Mag.	100 × 100 × 8	6.4%	13.8%
Mag.	100 × 100 × 10	6.1%	11.7%
Mag.	100 × 100 × 15	7.1%	18.0%
Mag.	200 × 200 × 15	23.5%	20.0%
Mag.	400 × 400 × 15	12.5%	18.8%

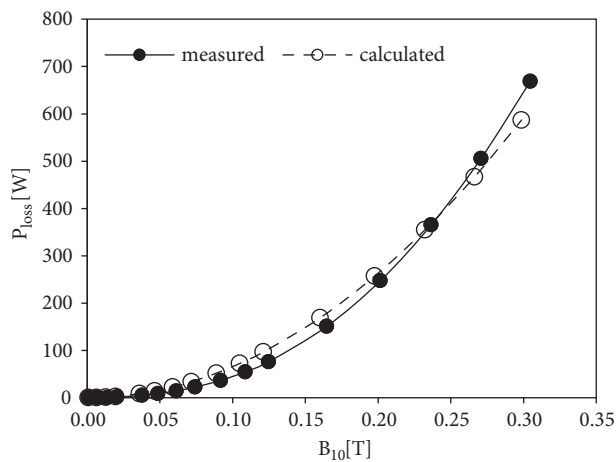


Figure 11. Measured and calculated losses in the magnetic steel sample with dimensions of 400 × 400 × 15 mm.

Table 9. Total and additional losses measured in sample transformers.

	Tr. A	Tr. B	Tr. C
Total losses [kW]	123.7 ± 1.5	435.1	528.9 ± 5.8
Additional losses [kW]	6.9 ± 0.3	17.4	81.8 ± 4

4.2. Finite-element models of transformers

The transformers are modeled in 3D FEM software as whole units because the high-voltage and low-voltage as well as top and bottom clearances are not equal. The windings are defined as hollow, conducting, stranded cylinders without leads. The core in the model is made of solid, nonlaminated, isotropic, linear, nonconductive material without hysteresis and with the real relative permeability of 20,000. Because of the model size, the surface impedance method was used to calculate losses. The tank and the clamping system are modeled as solid and linear materials whose electromagnetic properties (conductivity and relative complex permeability) have been taken from the equivalent properties of $400 \times 400 \times 15$ mm sample ($\mu'_r = 267.28$, $\mu''_r = 27.71$, $\sigma = 5.49 \times 10^6$ S/m). This sample was chosen because its geometry is the most similar to the concentrated field sources and large steel surfaces in the transformer. Transformers are observed in the state of short-circuit test. The short-circuit test condition is very suitable for calculating stray losses in the construction part because losses in the core and winding need not be calculated.

4.3. Results

Table 10 shows the components of losses in the clamping parts and tank for transformers A, B, and C. The rate of hysteresis losses relative to total losses is 9.4%.

Table 10. Power loss components in the clamping parts and tank in power transformers and ratio of hysteresis relative to the total additional losses.

	Losses [W]		
	Tr. A	Tr. B	Tr. C
Clamping ohmic	969.6	4387.6	15,543.1
Clamping hyst.	100.5	454.8	1611.3
Clamping total	1070.2	4842.5	17,154.3
Tank ohmic	279.1	312.3	3918.2
Tank hyst.	28.9	32.4	406.2
Tank total	308.0	344.6	4324.4
Total ohmic	1248.7	4699.9	19,461.2
Total hyst.	129.4	487.2	2017.4
Total	1378.2	5187.1	21,478.7
Hyst/total ratio	9.4%	9.4%	9.4%

Despite the optimization process used for finding the equivalent linear parameters of the magnetic steel, which yield the same measured and calculated losses in the physical model of the transformer core with the coil, the total additional losses calculated in the models of the actual power transformers differ considerably from the additional losses determined during the short-circuit test. A part of the reason for such variation certainly lies in the very simplified model, which does not contain leads, connecting wires, switches, and many smaller construction parts made of steel. The other reason for such deviation lies in the nature of the method for determination of additional losses. During the short-circuit test only the total losses are measured. From that value the ohmic losses, which are calculated from the measured current and previously measured winding resistance, are subtracted. Since ohmic losses form the majority of the total losses, even a small error in determination of ohmic losses represents a significant error in terms of additional losses. Finally, the value of skin-effect losses in the windings has to be subtracted from the total losses. That value cannot be measured and is typically calculated using a 2D rotational-symmetry model. Because of that, additional losses are mainly predicted statistically in the design stage while direct calculation of losses is used for investigation of local

overheating and prediction of losses in the case of special design interventions. For that reason it is important to realize that the hysteresis part of the losses in the steel caused by stray magnetic flux is not high and is approximately 9%. It is also important to note that the share of the hysteresis losses depends on the value of the real part of the complex permeability. Takahashi et al. [9] in the solution of TEAM Problem 21 found that the share of hysteresis losses for the real permeability of 1000 is around 17% for a steel plate of model B with a tendency to increase with the increase of the real permeability. In our case, the real permeability equals 267.28 and so the share of hysteresis losses is smaller than in [9].

5. Conclusion

This paper presents a method for determination of equivalent linear electromagnetic properties of nonlinear materials intended for calculation of losses in construction parts of power transformers using linear time-harmonic finite-element simulations. The method has been used to determine electric and magnetic properties of magnetic and nonmagnetic steel by combining a DE optimization algorithm and FEM simulation with the aim to reconstruct the losses in the nonlinear material using linear calculation in the limited range of flux density. For that purpose, a physical model of a transformer coil has been made. The model has been used to measure losses in the most direct manner in the samples made of copper and magnetic and nonmagnetic steel inserted into an air gap in the core. The flux density in the core has been varied from 0 to 0.6 T. Samples made of copper have been used for initial testing of the method since material properties of copper are well known.

For each sample made of magnetic and nonmagnetic steel, the equivalent specific conductivity and real relative permeability accompanied with imaginary relative permeability have been determined, which yield the same total eddy current and hysteresis losses in the volume of the sample as the measured ones. The results indicate that nonlinear magnetic material can be successfully substituted with linear magnetic material in the limited range of flux density in order to accomplish the same amount of losses. According to results, the equivalent real relative permeability of nonmagnetic steel is 3.50 and the equivalent specific conductivity is 7.86 MS/m, regardless of sample dimensions. The equivalent real and imaginary permeability of magnetic steel vary with sample dimensions due to strong nonlinearity of the material, but the equivalent specific conductivity is fairly constant with an average value of 5.76 MS/m. The nonlinearity of the material affects the magnetic field and eddy current distribution within its volume depending on the field source size relative to the size of the sample, which then affects the loss density and total losses within the sample.

This paper also presents the measurement of static magnetic characteristics and conductivity of magnetic and nonmagnetic steel. For magnetic steel a family of hysteresis curves, the first magnetization curve, and real and imaginary relative permeability curves are given.

Finally, the 3D FEM calculation of eddy current and hysteresis losses in the clamping parts and the tank of high-power transformers is presented. It has been determined that the hysteresis part of the losses in the steel caused by stray magnetic flux in the observed transformers is 9.4%. Due to dispersion of stray losses in various metallic parts of the transformers, which could not have been included in the FEM model, and the nature of the method for measurement of additional losses, which is in essence unreliable and extremely sensitive to errors, it was not possible to accurately calculate the total additional losses using linear 3D FEM time-harmonic simulation when compared to the measured values. Regardless of the problems with uncertainty of the measured additional losses in the power transformers, in all 3 cases the calculated losses are significantly lower than measured. This indicates that linear surface impedance even with hysteresis included cannot be used to correctly account for total losses in construction parts of the transformer regardless of the fact that it was possible to obtain the equality of thus calculated and measured losses on a small-scale sample made of

magnetic steel. The main contribution of this paper is the establishment of the level of reliability of the linear surface impedance method for calculation of stray losses in solid magnetic steel parts of power transformers. The conclusions drawn from the experimental data and 3D FEM models can be also applied for other electromagnetic devices with parts made of solid nonmagnetic or magnetic material that are exposed to sinusoidally varying magnetic fields. It is possible to find the equivalent linear magnetic properties of the inherently nonlinear material to reliably calculate the stray losses, which has been confirmed by experiments conducted on samples inserted into a transformer core model with a coil.

References

- [1] Karsai K, Kerenyi D, Kiss L. Large Power Transformers. New York, NY, USA: Elsevier, 1987.
- [2] Štrac L. Determination of electromagnetic properties of steel for prediction of additional losses in power transformers. PhD, University of Zagreb, Zagreb, Croatia, 2011.
- [3] Weber C, Fajans J. Saturation in nonmagnetic stainless steel. *Rev Sci Instrum* 1998; 69: 3695–3697.
- [4] Basak A, Rowe DM, Anayi FJ. Magnetic flux and loss measurement using thin film sensors. *IEEE T Magn* 1995; 31: 3170–3172.
- [5] Basak A, Rowe DM, Anayi EJ. Thin film senses flux and loss in machines. In: Proceedings of the UK Magnetics Society Seminar, p. 12, 1994.
- [6] Birkfeld M, Hempel KA. A new field-sensing method to measure the power loss of electrical steel sheet under two-dimensional measuring conditions. *IEEE T Magn* 1996; 32: 4908–4910.
- [7] Skutt GR. High-frequency dimensional effects in ferrite-core magnetic devices. PhD, Virginia Polytechnic Institute and State University, Blacksburg, VA, USA, 1996.
- [8] Storn R, Price K. Differential evolution - A simple and efficient heuristic for global optimization over continuous space. *J Global Optimization* 1997; 11: 341–359.
- [9] Takahashi N, Sakura T, Cheng Z. Nonlinear analysis of eddy current and hysteresis losses of 3-D Stray field loss model (Problem 21). *IEEE T Magn* 2001; 37: 3672–3675.